PHYSICAL REVIEW B VOLUME 28, NUMBER 9 1 NOVEMBER 1983

Paramagnetic resonance of Gd^{3+} as a probe of exchange and crystal-field effects in rare-earth-metal pnictides: Antiferromagnetic and diluted materials

K. Sugawara*
Department of Physics, Case Western Reserve University, Cleveland, Ohio 44106

C. Y. Huang
Los Alamos National Laboratory, Los Alamos, New Mexico 87545

Bernard R. Cooper
Center for Materials Science, Los Alamos National Laboratory, Los Alamos, New Mexico 87545
and Department of Physics, West Virginia University, Morgantown, West Virginia 26506†
(Received 30 August 1982; revised manuscript received 20 July 1983)

We have extended the previous study of electron paramagnetic resonance (EPR) of dilute Gd^{3+} impurities in Van Vleck paramagnets to study related antiferromagnetic compounds. The host systems studied are the terbium monopnictides and the cerium monopnictides. We have studied both pure host systems and systems with the host rare-earth metal diluted with yttrium. Since the Gd^{3+} EPR linewidths are often substantial compared to the resonance field, we have included the antiresonance (negative-frequency) effect in the analysis. The Gd^{3+} resonance g factor serves to probe the host susceptibility. Of particular interest in this regard is the g-factor behavior for TbP as the host system. This agrees quite closely with the superconducting quantum interference device magnetometer susceptibility behavior (i.e., in extremely small magnetic field) found by Kötzler *et al.*, showing that the EPR g factor obtained indeed measures the linear response of the host system. This effect should be useful for studying systems such as CeSb where the apparent susceptibility, as conventionally measured, is likely to include substantial nonlinear contributions. The linewidth behavior is complex. Fluctuation effects among host crystal-field levels sometimes dominate, and this allows the host crystal-field splitting to be determined.

I. INTRODUCTION

Previously we have reported[1] on the use of electron paramagnetic resonance (EPR) of dilute Gd^{3+} impurities as a probe of exchange and crystal-field effects in the Van Vleck paramagnets TmX and PrX (where X is one of the group-VA elements P, As, Sb, and Bi), i.e., the thulium and praseodymium monopnictides of NaCl structure. The information obtained resulted from the fact that the resonance g values and linewidths of the Gd^{3+} impurities serve to probe the behavior of the isothermal and repopulation susceptibilities of the host materials, respectively. (The isothermal susceptibility is the susceptibility measured under circumstances where the spin system remains in thermal equilibrium with the lattice during the measurement period. The repopulation susceptibility is the difference between the isothermal and the isolated susceptibilities. The isolated susceptibility is that measured when the thermal populations of the levels do not change, i.e., the effect measured is due to the change in wave functions, and hence moments, with field, the polarization effect.)

In the present work we have extended this study to related antiferromagnetic compounds, the cerium monopnictides and the terbium monopnictides. The Gd^{3+} EPR has been followed as a function of temperature on traversing the Néel temperature (T_N). In addition, we have studied the behavior of the Gd^{3+} EPR in these materials on diluting the magnetic rare-earth constituent of the host with yttrium. Since terbium has a singlet crystal-field ground state, when the terbium is diluted sufficiently, the material no longer orders magnetically at any temperature,[2] i.e., it becomes a Van Vleck paramagnet. All the materials studied have NaCl structure.

The most interesting result of the present study is the Gd^{3+} EPR g-factor behavior on traversing T_N. One would expect the g-factor behavior to reflect the host susceptibility behavior because of the exchange interaction between the Gd^{3+} ion and the host rare-earth ions. If the Gd^{3+} is weakly exchange coupled to the host rare-earth ions and if that Gd^{3+} to Ce^{3+} or Tb^{3+} exchange is sufficiently long range, then a reasonable expectation would be a "g shift" of the Gd^{3+} EPR with a temperature dependence reflecting that of the host isothermal susceptibility. Apparently this situation of weak, rather long-range, Gd^{3+}-host rare-earth exchange is that prevailing for Gd^{3+} in the cerium and terbium monopnictides, since the experimental g shift reflects the isothermal susceptibility. Also, the experimental results indicate that the moment fluctuations of the host ion among crystal-field levels sometimes determine the linewidth of the Gd^{3+} EPR. However, the linewidth behavior as discussed below is complex.

The experimental g factor and linewidth behavior is presented in Sec. II and discussed in Sec. III. The fact

 ©1983 The American Physical Society

that the linewidths for the materials studied are typically substantial compared to the resonance field has led us to include both positive- and negative-frequency effects in the analysis used in Sec. II (details in the Appendix). Some concluding remarks are given in Sec. IV.

II. EXPERIMENTAL BEHAVIOR

In an EPR experiment one conventionally observes the first derivative of power absorbed for varying dc field at fixed microwave frequency. In a metallic sample, this power absorption is proportional to a mixture of $\chi'(H)$ and $\chi''(H)$, the dispersive and absorptive parts of the dynamic susceptibility. Special care must be taken to extract the resonant field and linewidth from the raw data when these two quantities are comparable and the microwave magnetic field is linearly polarized. This is because not only the positive, but also the negative, frequency component of the dynamic susceptibility, i.e., both the resonance and antiresonance terms in the line-shape function, must be taken into account in considering the microwave power absorbed. To do this we have adopted a graphical procedure. This deals with the problem that the recorded signal is dP/dH; and since dP/dH does not vanish as H vanishes, the resonance field is not the field at which dP/dH has the same value as at $H=0$.

We have defined five parameters corresponding to easily identified fields or amplitudes for a given set of experimental data; using conventional analysis,[3-6] we have generated curves giving a unique set of these five parameters for each resonance field H_0 and linewidth DH. Thus for any set of data we have extracted H_0 and DH by comparing the experimental values for our five parameters to the reference curves. Some details of this procedure are given in the Appendix.

Once H_0 and DH have been obtained [as well as a coefficient giving the mixing between $\chi'(H)$ and $\chi''(H)$ in the power absorption], one can check the overall quality of fit with the experimental dP/dH behavior. In general, we have found the fit is quite good. We have found that the experimentally observed peak-to-peak linewidth ΔH_{pp} is close to the true linewidth DH, differing by a constant factor ~ 1.4 for varying temperatures in a given case. Therefore, in presenting the experimental linewidth behavior we show the peak-to-peak linewidths.

The powder samples used in this work were prepared according to a method similar to the one described in Ref. 1. The EPR spectra were obtained with a conventional EPR spectrometer operated at 9.2 GHz.

In this section we present the experimental results for the Gd^{3+} EPR behavior with terbium monopnictides and cerium monopnictides as hosts. The main discussion of this experimental behavior follows in Sec. II.

A. Terbium monopnictides

The g values for the Gd^{3+} EPR in the $Tb_\zeta Y_{1-\zeta}P$ hosts are shown in Fig. 1. For undiluted TbP, the g value peaks at 8 K. This is the value of T_N from susceptibility measurements.[7] For $Tb_{0.5}Y_{0.5}P$ and $Tb_{0.1}Y_{0.9}P$ as host, the g-value behavior is as expected for a Van Vleck paramagnet.[1]

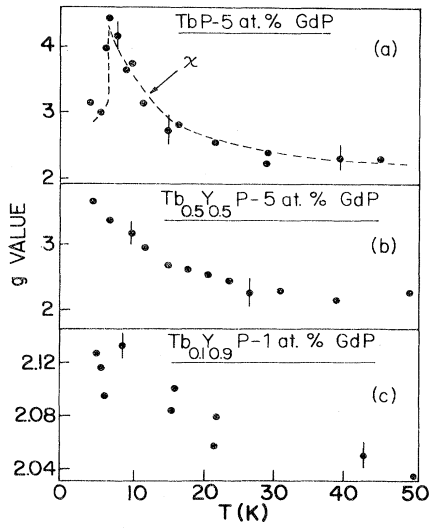

FIG. 1. Temperature dependence of Gd^{3+} EPR g values in TbP, $Tb_{0.5}Y_{0.5}P$, and $Tb_{0.1}Y_{0.9}P$. Experimental behavior of the susceptibility χ found by Kötzler *et al.* (Ref. 14) for TbP is shown by the dashed curve in the upper panel.

The EPR linewidth for Gd^{3+} in $Tb_\zeta Y_{1-\zeta}P$ is shown in Fig. 2. For $\zeta=1.0$ and 0.5 the linewidth increases as a function of temperature. For $\zeta=0.1$, on the other hand, the linewidth decreases as a function of temperature.

As shown in Fig. 3, the g value for Gd^{3+} in $Tb_\zeta Y_{1-\zeta}As$ for $\zeta=0.8$, 0.5, and 0.3 decreases with increasing T. This is consistent with our expectation that for $\zeta=0.5$ and 0.3 these are Van Vleck paramagnets, and for $\zeta=0.8$, the Néel temperature ($T_N=9$ K) is quite low. The Gd^{3+} linewidth in pure TbAs is too broad for the g value to be determined. (For[8] TbAs, $T_N=10.5$ K.)

The temperature variation of the linewidth for the Gd^{3+} EPR in TbSb and in $Tb_\zeta Y_{1-\zeta}As$ with $\zeta=1$, 0.8, 0.5, 0.3, and 0.1 is shown in Fig. 4. For pure TbAs and TbSb the linewidth decreases with increasing T. For

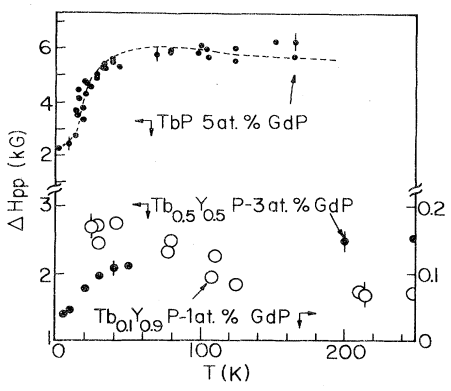

FIG. 2. Temperature dependence of peak-to-peak linewidths of Gd^{3+} EPR in TbP, $Tb_{0.5}Y_{0.5}P$, and $Tb_{0.1}Y_{0.9}P$. Dashed curve drawn through the data points for TbP is the theoretical curve using Eq. (4). In the lower part of the figure, solid circles show the data for $Tb_{0.5}Y_{0.5}P$, and open circles show the data for $Tb_{0.1}Y_{0.9}P$.

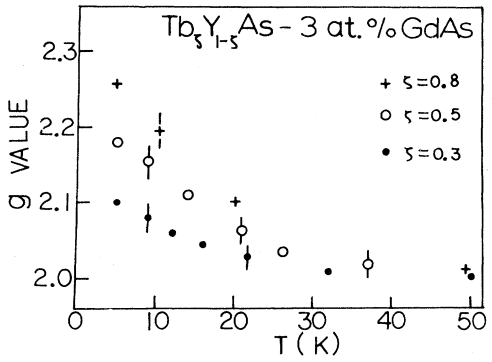

FIG. 3. Temperature dependence of Gd^{3+} EPR g values in $Tb_{0.8}Y_{0.2}As$, $Tb_{0.5}Y_{0.5}As$, and $Tb_{0.3}Y_{0.7}As$.

$Tb_\zeta Y_{1-\zeta}As$, the most interesting feature of the linewidth behavior is the increase with temperature for $\zeta=0.8$, compared to the decrease with temperature for pure TbAs and a slight decrease with T for lower values of ζ.

B. Cerium monopnictides

The Gd^{3+} EPR g values for CeP ($T_N=10$ K, CeAs ($T_N=8$ K), and CeSb ($T_N=16$ K) are shown in Fig. 5 for a range of temperature including T_N. The linewidth behavior for Gd^{3+} in CeP, CeAs, and CeSb is shown in Fig. 6. Unlike the Van Vleck paramagnetic materials studied earlier,[1] the linewidth behavior cannot be described by simple theory based on fluctuation effects among the host crystal-field levels.

We have also studied the EPR of Gd^{3+} in CeX diluted by nonmagnetic yttrium. As shown in Fig. 7, the linewidth decreases somewhat with temperature, flattening out at temperatures of about 40 K. The Néel temperatures of these materials are quite low, so that the question arises as to whether there is another mechanism (such as dipole-dipole interaction) other than critical fluctuations

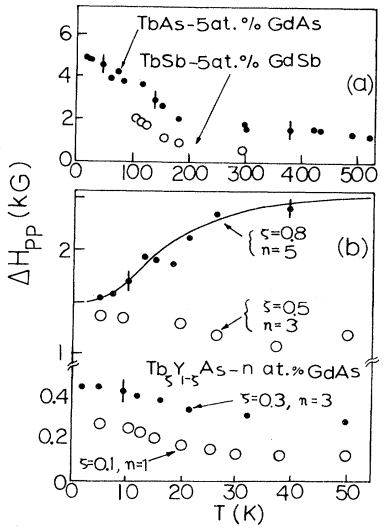

FIG. 4. Temperature dependence of peak-to-peak linewidth of Gd^{3+} EPR in TbSb, TbAs, $Tb_{0.8}Y_{0.2}As$, $Tb_{0.5}Y_{0.5}As$, $Tb_{0.3}Y_{0.7}As$, and $Tb_{0.4}Y_{0.9}As$. Solid curve is obtained using Eq. (4).

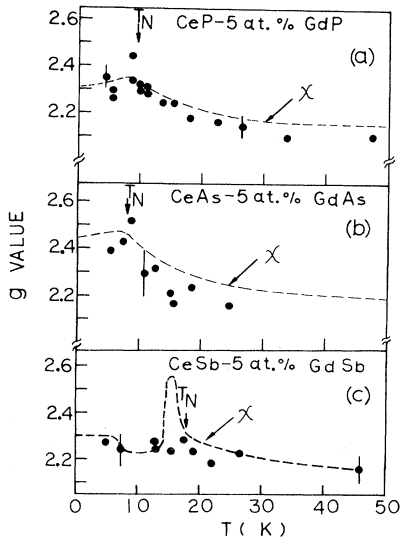

FIG. 5. Temperature dependence of g value for Gd^{3+} EPR in CeP, CeAs, and CeSb compared to susceptibility behavior of Ref. 21. See text (Sec. III) for discussion of CeSb susceptibility. Susceptibility behavior is shown in arbitrary units.

or fluctuations among crystal-field levels, dominating the behavior at lower temperatures when the crystal-field doublet ground state is predominately occupied. Particularly noteworthy is the change in behavior from CeP to $Ce_{0.3}Y_{0.7}P$.

III. DISCUSSION

We will first discuss the experimental results for the terbium monopnictides as hosts, and then those for the cerium monopnictides.

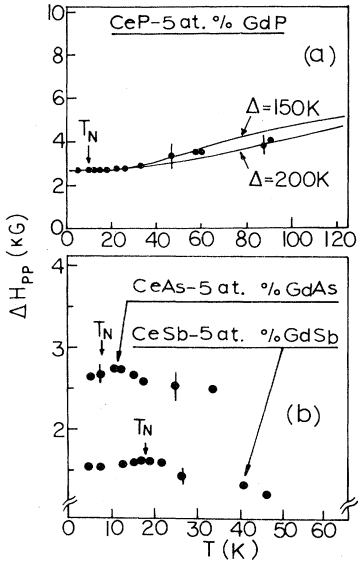

FIG. 6. Temperature dependence of peak-to-peak linewidth for Gd^{3+} EPR in CeP, CeAs, and CeSb. For CeP, the fit to data using Eq. (4) with $\Delta=150$ and 200 K is indicated (solid curves).

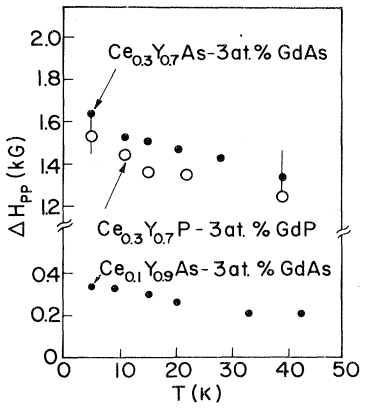

FIG. 7. Temperature dependence of peak-to-peak linewidth for Gd^{3+} EPR in $Ce_{0.3}Y_{0.7}As$, $Ce_{0.3}Y_{0.7}P$, and $Ce_{0.1}Y_{0.9}As$.

A. Terbium monopnictides

The g shift for the Gd^{3+} EPR caused by exchange interaction with a paramagnetic ion is given by[1]

$$\Delta g=\frac{\lambda-1}{\lambda}\frac{J(0)}{\mu_B^2}\chi\ , \tag{1}$$

where λ is the Lande g factor of the host,

$$J(0)=\sum_j J_{ij} \tag{2}$$

is the exchange between the impurity Gd^{3+} ion and all host ions, and χ is the experimental susceptibility in which the host-host exchange enhancement of the susceptibility is included.

$Tb_\zeta Y_{1-\zeta}P$ is a singlet ground-state antiferromagnetic system quite similar to $Tb_\zeta Y_{1-\zeta}Sb$, the susceptibility behavior of which has been extensively studied by Cooper and Vogt.[2] For ζ below some critical value, just as with[2] $Tb_\zeta Y_{1-\zeta}Sb$, the system will become a Van Vleck paramagnet. We expect $\zeta=0.5$ to be close to or below the critical value.

For $Tb_{0.5}Y_{0.5}P$ and $Tb_{0.1}Y_{0.9}P$ as hosts, as seen from Fig. 1, the experimental g-value behavior is as expected for a Van Vleck paramagnet. Using Eq. (1), from the $Tb_{0.5}Y_{0.5}P$ behavior we deduce a Gd-Tb exchange, $J(0)=8\pm1$ K.

Provided that the EPR linewidths of the host rare-earth ion are greater than that of the Gd^{3+} EPR, then the spin fluctuations of the host, felt through the host-Gd^{3+} exchange, are the determining factor in the Gd^{3+} linewidth.[9] When these fluctuations are dominated by the host crystal-field interaction, the linewidth of the Gd^{3+} EPR is given by[1,10]

$$\Delta H=AkT(\chi_T-\chi_{\rm iso})\equiv AkT\chi_R\ , \tag{3}$$

where χ_T and $\chi_{\rm iso}$ are the isothermal and isolated susceptibilities of the host, as discussed in the Introduction, and $\chi_R\equiv\chi_T-\chi_{\rm iso}$ is[1,11] the repopulation contribution to the susceptibility. This gives

$$\begin{aligned}\Delta H=A\{&\langle\Gamma_{4a}\,|\,J_z\,|\,\Gamma_{4a}\rangle^2\exp[-E(\Gamma_4)/kT]\\&+\langle\Gamma_{5a}^{(2)}\,|\,J_z\,|\,\Gamma_{5a}^{(2)}\rangle^2\exp[-E(\Gamma_5^{(2)})/kT]\\&+\langle\Gamma_{5a}^{(1)}\,|\,J_z\,|\,\Gamma_{5a}^{(1)}\rangle^2\exp[-E(\Gamma_5{}^{(1)})/kT]\}/Z\end{aligned} \tag{4}$$

(for Gd^{3+} in $Tb^{3+}X$).

As seen in Fig. 2, the EPR linewidth for the Gd^{3+} resonance in the $Tb_\zeta Y_{1-\zeta}P$ hosts for $\zeta=1.0$ and 0.5 increases with increasing temperature. Thus the behavior for $Tb_{0.5}Y_{0.5}P$ is that expected for a Van Vleck paramagnet when fluctuations within crystal-field levels determine the Gd^{3+} EPR linewidth [i.e., under conditions given by Eqs. (3) and (4)]. On the other hand, for $\zeta=0.1$ the Gd^{3+} EPR linewidth decreases with increasing temperature. Presumably this occurs because the EPR linewidth of Tb^{3+} in $Tb_{0.1}Y_{0.9}P$ is narrower than those of $\zeta=1.0$ and 0.5, so that the conditions leading to Eq. (4) do not apply (the coupling to the Tb^{3+} ion no longer is the dominant relaxation route for the Gd^{3+} ions).

For $Tb_{0.5}Y_{0.5}P$, where the conditions yielding Eq. (4) appear to be satisfied, one can use Eq. (4) to fit the data and obtain a value for $\Delta=E(\Gamma_4)-E(\Gamma_1)$, the crystal-field splitting to the first excited crystal-field level of the level scheme for Tb^{3+} shown in Fig. 8. The crystal-field level scheme for Tb^{3+} depends on x, the parameter[12] giving the ratio of fourth- to sixth-order crystal-field anisotropy (because of the presence of two levels of Γ_5 symmetry). Therefore, as shown in Fig. 9, the theoretical temperature dependence of the linewidth of the Gd^{3+} EPR in paramagnetic TbX given by Eq. (4) depends on x. By comparing the curves given in Fig. 9 with the data for $Tb_{0.5}Y_{0.5}P$ given in Fig. 2, we can obtain Δ as well as x with about 15% accuracy. The Δ and x values obtained are 18 K and -0.85 ± 0.15. The Δ value is close to the value obtained from microwave resistivity measurements[13] on TbP.

In Ref. 1, Eq. (1) was derived for the paramagnetic regime in the host material. The appropriateness of using Eq. (1) in the host antiferromagnetic regime depends on

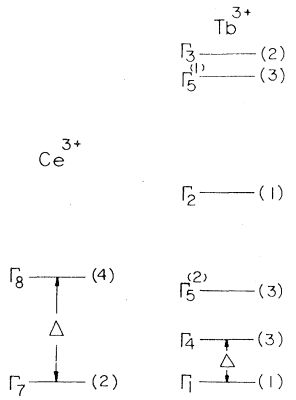

FIG. 8. Crystal-field energy levels for Ce^{3+} and Tb^{3+} in octahedral environment. Situation for Tb^{3+} is that when fourth-order crystal-field anisotropy is dominant.

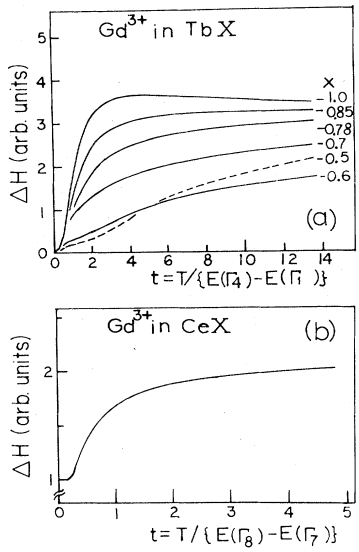

FIG. 9. Theoretical dependence of Gd^{3+} linewidth from Eqs. (4) and (5) of text.

how strongly the Gd^{3+} moment is coupled to the host system. Observation of a well-defined Gd^{3+} resonance for Gd^{3+} in TbP in the host antiferromagnetic regime implies that the coupling is rather weak, i.e., Gd^{3+} acts as a (weakly exchange coupled to the lattice) localized magnetic impurity mode. Then it is reasonable to adopt a picture where the temperature-dependent g shift gives the linear response (i.e., the susceptibility in the limit of vanishing applied magnetic field) of the host to the ac field imposed (via Gd-Tb exchange) on the host by the Gd^{3+} under resonance conditions. If the Gd-Tb exchange is relatively long range, then the Gd^{3+} is sampling the spatially averaged linear response of the host, and the temperature dependence of the g factor provides a measure of the susceptibility as conventionally defined, i.e., it is appropriate to use Eq. (1). [Note that the importance of the range of the Gd-Tb exchange in justifying the validity of Eq. (1) is the same as in the case of a paramagnetic host.] In Fig. 1, we also show the "zero-field" susceptibility [measured in the earth's magnetic field using a superconducting quantum interference device (SQUID) magnetometer] measured by Kötzler *et al.*[14] The excellent agreement of the susceptibility behavior with the g-factor behavior supports our hypothesis for the validity of using Eq. (1) below T_N when a well-defined Gd^{3+} resonance is observed.

As can be seen from Fig. 4, for $Tb_\zeta Y_{1-\zeta}As$ the changeover in dominant relaxation mechanism already noted for $Tb_\zeta Y_{1-\zeta}P$ apparently occurs at higher Tb concentration, between $\zeta=0.8$ and 0.5, as indicated by the change in the temperature dependence of the linewidth from increasing to decreasing with increasing temperature. More puzzling is the difference in linewidth behavior for TbP, which increases with temperature up to about 50 K (see Fig. 2), compared to TbAs, which decreases significantly with temperature up to 150 or 200 K (see Fig. 4). (The behavior for TbSb, also shown in Fig. 4, has been followed only above 100 K. There is no strong contrast in the linewidth behavior of the three terbium pnictides in this higher-temperature range.) The Néel temperatures for TbP and TbAs are quite similar, 8 K compared to 10.5 K; therefore, effects associated with exchange do not seem to offer an explanation. Perhaps the difference lies in the difference of the electronegativity (affecting conductivity) or mass (affecting phonon behavior and elasticity) of the anion. If this behavior of pure TbAs does not affect the interpretation of the $Tb_{0.8}Y_{0.2}As$ behavior, using Eq. (4) and the temperature dependence of ΔH_{pp} in $Tb_{0.8}Y_{0.2}As$ one deduces $\Delta=E(\Gamma_4)-E(\Gamma_1)=14-18$ K and $x=-(0.95-1.00)$ for TbAs, quite reasonable values.

B. Cerium monopnictides

Currently there is great interest in the magnetic behavior of the cerium monopnictides. The highly unusual magnetic behavior of CeSb and CeBi can be understood[15,16] on the basis of a highly anisotropic Ce-Ce interaction mediated via hybridization with the band electrons. Such an interaction gives rise to a situation where there are a number of states of the magnetic system corresponding to a variety of magnetic structures, which lie quite close in energy to one another compared to the overall energy of magnetic ordering. Thus one has transitions over a narrow range of temperature and field between quite different magnetic structures. Also, one has a strong possibility of metastable behavior, and this is consistent with the observation[17–19] of considerable hysteresis and magnetic remanence in the lower-temperature magnetically ordered phases of CeBi and CeSb.

For CeSb and CeBi, the crystal-field splitting is smaller than or comparable to the anisotropic Ce-Ce exchange. This can be seen by comparing Néel temperatures and crystal-field splittings[20] (between the Γ_7 doublet and the Γ_8 quartet). For CeBi, $T_N=25$ K and $\Delta\approx 10-15$ K; while for CeSb, $T_N=16$ K and $\Delta=25$ K. On the other hand, for CeP and CeAs, as indicated by comparing Δ and T_N, the crystal-field splitting is much larger than the anisotropic exchange ($\Delta=150-200$ K, while $T_N=8$ to 10 K). Thus we expect the metastability associated with the anisotropic exchange to be absent in CeP and CeAs.

It is interesting to consider the g-factor behavior in Fig. 5 in relation to this question of metastability and associated magnetic hysteresis and remanence. For Gd^{3+} in CeP and CeAs the correlation of the temperature dependence of the g factor with the experimental susceptibility seems to be present, much as it is for TbP in Fig. 1. On the other hand, for CeSb the g factor shows little correlation with the susceptibility as originally measured[21] (dashed curve shown in the lower panel of Fig. 5). However, the way that these susceptibility measurements were done (standard technique at that time—cooling in a rather high field of approximately 10 kOe, where $\chi\equiv M/H$, with H equal to that field) introduced two features into the χ-vs-T behavior that, on the basis of subsequent information, we can recognize as artifacts. These are (1) the pronounced maximum and shallow minimum covering the region from about 20 K to 8 K, and (2) the rise and flattening from 8 K through the lowest temperatures. The basis for both these artifacts lies in the many closely lying (in energy) phases for CeSb for varying H and T in the magneti-

cally ordered regime and the associated tendency toward metastability.

We first discuss the origin of feature (1) in the χ-vs-T behavior for CeSb of Ref. 21 as reproduced in Fig. 5. The neutron-diffraction measurements of Rossat-Mignod *et al.*[19] show a ferromagnetic phase (labeled FP_1 in their Figs. 3 and 4) dipping down to a field of about 5 kOe at its low point and extending over the temperature range around $T_N = 16$ K. The transition into this phase induced by a magnetic field of more than 4 or 5 kOe for temperatures close to T_N is also shown in the magnetization measurements of Bartholin *et al.*[18] and is graphically illustrated in the "three-dimensional" drawing in their Fig. 2. The measurements of Ref. 21 giving the χ reproduced in Fig. 5 were done in a field of approximately 10 kOe (a reasonable procedure on the basis of the then existing information), so that feature (1) really represents the nonlinear response involved in the transition into the FP_1 phase. The g-factor values shown in Fig. 5 correspond to fields below that triggering the FP_1 transition since the resonance field is about 3 kOe, and the measurements determining the fitting were those for fields up to 1 or 2 kOe above that value.

Feature (2) in the χ curve for CeSb reproduced from Ref. 21 in Fig. 5 (the rise and flattening below 8K) can be understood on the basis of the metastability and associated thermoremanence below 8 K in CeSb as reported by Bartholin *et al.*[17] The effects of this thermoremanence can be seen by considering Fig. 10 which gives the corresponding behavior for CeBi. This shows thermoremanence below 12 K. (As far as we know, a figure for CeSb corresponding to Fig. 10 for CeBi does not exist. Fig. 10 was reported in the talk corresponding to Ref. 17, but has not been previously published. It is shown here through the courtesy of H. Bartholin and I. S. Jacobs.) If the magnetization measurements giving χ are done by cooling in substantial field, one gets an artificially high apparent χ associated with thermal remanence. Our own EPR measurements were done by cooling in zero field, i.e., the field was cycled up and down at each temperature. However, in any case, our data do not extend to low enough temperature and the scatter of points is such that it cannot be ascertained whether the g factor comes in flat to zero temperature or shows a slight rise.

In summary, we feel that the temperature-dependent g behavior of CeSb shown in Fig. 5 probably reflects the intrinsic very-low-field (i.e., linear response) susceptibility in the same way as the g-factor behavior shown in Fig. 1 does for TbP.

Perhaps coincidentally, the linewidth behavior for the cerium monopnictides gives some indication of the same qualitative trend already commented on above for the terbium monopnictides. For the phosphide there is a small increase with temperature, while the arsenide and antimonide show slight decreases above T_N. If the behavior in CeP can be associated with fluctuations among the host crystal-field levels, then we can use the theory of Eq. (3) to find the crystal-field splitting,

$$\Delta H = B\{\langle\Gamma_7|J_z|\Gamma_7\rangle^2\exp[-E(\Gamma_7)/kT] + (\langle\Gamma_{8a}|J_z|\Gamma_{8a}\rangle^2+\Gamma_{8b}|J_z|\Gamma_{8a}\rangle^2) \times\exp[-E(\Gamma_8)kT]\}/Z \quad (5)$$

(for Gd^{3+} in CeX), where the subscripts a and b denote individual states of the Zeeman split degenerate states, and Z is a single-ion crystal-field partition function. (For Ce^{3+} the situation is somewhat complicated, because the contribution to χ_R from the excited Γ_8 quartet depends on the direction of the magnetic field. However, our calculations show that the dependence of ΔH on direction of H is not strong; so we show Δ for H along a $\langle 100\rangle$ direction in Fig. 9.) As shown in Fig. 6, this gives a crystal-field splitting of 150 to 200 K in agreement with the results of the neutron scattering measurements of Heer *et al.*[20]

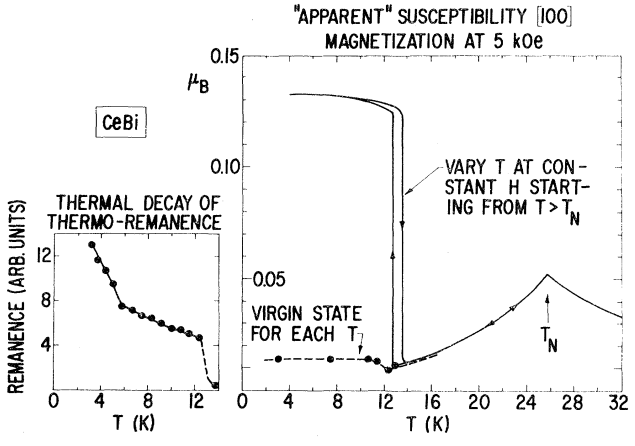

FIG. 10. Susceptibility and thermoremanence of CeBi. See discussion in Sec. III of text. (Figure was reported in talk corresponding to Ref. 17 but has not been previously published. This figure is published here through the courtesy of H. Bartholin and I. S. Jacobs.)

IV. CONCLUDING REMARKS

The Gd^{3+} EPR, through the g-factor behavior, has proved to be a good probe of the host isothermal susceptibility. The g-factor behavior can be used to determine the Gd-host (a different rare earth) exchange value both in paramagnetic and antiferromagnetic systems.

The Gd^{3+} EPR linewidth behavior in the antiferromagnetically ordered cerium and terbium monopnictides is quite complex. The expressions in Eqs. (4) and (5) give the linewidth in idealized situations. In addition, for systems that order magnetically or that have host rare-earth concentrations near to values necessary for magnetic ordering, there may be important effects associated with the critical fluctuations of the host. Other effects, such as dipole-dipole interactions may contribute (potentially more important for Ce^{3+} which has a non-Kramers crystal-field ground state.) These additional effects, which depend on host-host coupling, may give complex behavior of the linewidth with host concentration when the host is diluted with a nonmagnetic diluent such as yttrium. The distinctive characteristic of the crystal-field-

dominated linewidth seems to be the monotonic increase with temperature, at low temperature, expected for this mechanism. When this increase is absent, we assume that another mechanism is serving as the dominant "bottleneck" in the relaxation processes. When the linewidth increases with temperature we assume that the fluctuation effect among crystal-field levels of the host dominates the linewidth behavior, and we have been able to deduce the crystal-field splitting of the host. However, at times fluctuation effects associated with magnetic ordering play an important role, obviating the possibility of such analysis; there are also effects dependent on the host concentration in systems diluted with yttrium that are not fully understood.

ACKNOWLEDGMENTS

Suggestions of D. L. Huber have been valuable in emphasizing the importance of inclusion of the antiresonance contribution for a correct analysis of the data. We have also benefited from discussions with J. Lawrence. The work of C.Y.H. and B.R.C. at Los Alamos National Laboratory was performed under the auspices of the U. S. Department of Energy. The work of B.R.C. at West Virginia University was supported by the National Science Foundation under Grant No. DMR-82-04261.

APPENDIX: LINE SHAPE AND ANALYSIS TO OBTAIN g VALUE AND LINEWIDTH

Taking account of both positive- and negative-frequency components, the average power absorbed per unit volume as a function of dc field is

$$P(H)\propto\left[\frac{H/DH}{1+[(H-H_0)/DH]^2}+\frac{H/DH}{1+[(H+H_0)/DH]^2}\right]+b_0\left[\frac{-(H/DH)[(H-H_0)DH]}{1+[(H-H_0)/DH]^2}+\frac{(H/DH)[(H+H_0)/DH}{1+[(H+H_0)/DH]^2}\right], \tag{A1}$$

where H_0 and DH are the resonant field and the linewidth, i.e., half-power half-width introduced by Peter *et al.*,[5] respectively. Here b_0 is a parameter, giving the admixture of the absorptive and dispersive parts of the dynamic susceptibility, which depends upon the metallic nature of the sample and on the experimental conditions in a complicated way.

Expression (A1) follows directly from the conventional linearized treatment of the Bloch equations, including both the resonance and the antiresonance terms.[6] The second term in each of the large parentheses gives the negative-frequency contribution to $P(H)$. [We note that $P(H)$ is an even function of H, i.e., for H and H_0 the absolute values are to be used. Also by gathering together terms in Eq. (A1), one can see that $P(H)$ is always positive.] The derivative of power absorbed for varying H can easily be obtained from Eq. (A1) to give

$$\frac{dP}{dH}\propto\left[\frac{(1-X^2)-2C_0X}{(1+X^2)^2}+\frac{1-X(X+2C_0)}{[1+(X+2C_0)^2]^2}\right]-b_0\left[\frac{C_0(1-X^2)+2X}{(1+X^2)^2}+\frac{C_0[1-(X+2C_0)^2]-2(X+2C_0)}{[1+(X+2C_0)^2]^2}\right], \tag{A2}$$

with

$$X\equiv\frac{H-H_0}{DH}, \tag{A3}$$

$$C_0\equiv\frac{H_0}{DH}. \tag{A4}$$

The typical line shape corresponding to Eq. (A2) is shown in Fig. 11. From Eqs. (A1) and (A2) we can see that the power absorbed is zero[22] when $H=0$, but dP/dH is nonzero at $H=0$. Thus there is the matter of establishing the true zero base line corresponding to zero power absorption when the recorded signal is actually dP/dH, i.e., the resonance field is not the field at which dP/dH has the same value as at $H=0$.

Obtaining the resonance field H_0 and the linewidth DH involves analyzing the line-shape data in a typical case, such as is shown in Fig. 11, in order to relate the data to the theoretical expression in Eq. (A2). This requires analyzing the experimental data for each case in such a way as to obtain values for the parameters b_0 and C_0 of Eq. (A2), and an additional parameter C_r defined in Fig. 11, which locates the resonance field H_0 relative to the minimum in dP/dH.

To do this we have adopted a graphical procedure. We define five parameters, a, b, d, A', and B' as shown in Fig. 11, corresponding to easily identified fields or amplitudes for a given set of experimental data. Then for a number

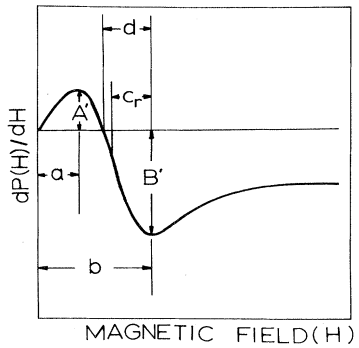

FIG. 11. Typical line shape with definition of parameters used in analysis.

of sets of specified b_0, C_0, and C_r values, we generate curves using Eq. (A2), i.e., one curve for each set of b_0, C_0, and C_r. This then gives us a set of a, b, d, A', and B' (actually the ratio A'/B') corresponding to each b_0, C_0, and C_r.

In this way we generate five reference curves (available upon request). Then a given set of experimental data provides values for a/b, d/b, A'/B', and b, and then by use of these curves we find that b_0, C_0, and C_r values consistent with these experimental parameter values.

---

*Present address: Research Administration, Engineering Center, Sharp Corporation, Nara 632, Japan.

†Permanent address.

[1]K. Sugawara, C. Y. Huang, and B. R. Cooper, Phys. Rev. B 11, 4455 (1975).

[2]B. R. Cooper and O. Vogt, Phys. Rev. B 1, 1218 (1970).

[3]G. E. Pake, *Paramagnetic Resonance* (Benjamin, New York, 1962).

[4]For example, see J. H. Pifer and R. Magno, Phys. Rev. B 3, 663 (1971).

[5]M. Peter, D. Shaltiel, J. H. Wernick, H. J. Williams, J. B. Mock, and R. C. Sherwood, Phys. Rev. 126, 1395 (1962).

[6]For example, R. M. White, *Quantum Theory of Magnetism* (McGraw-Hill, New York, 1970), pp. 121 and 122.

[7]G. Busch, P. Schwob, O. Vogt, and F. Hulliger, Phys. Lett. 11, 100 (1964).

[8]G. Busch, O. Vogt, and F. Hulliger, Phys. Lett. 15, 301 (1965).

[9]One of us (K.S.), has shown [Ph.D. thesis, Case Western Reserve University, 1975 (unpublished)] that for $Gd_xY_{1-x}As$ with $x=0.01$ and 0.03, the linewidths are ~ 50 G and ~ 180 G respectively, and they are temperature independent for $T<100$ K. Thus it appears that linewidth contributions from dipole-dipole or Ruderman-Kittel-Kasuya-Yosida (RKKY) interactions for the systems considered would be both small and temperature independent.

[10]T. Moriya and Y. Obata, J. Phys. Soc. Jpn. 13, 1333 (1958).

[11]B. R. Cooper, R. C. Fedder, and D. P. Schumacher, Phys. Rev. Lett. 18, 744 (1967); B. R. Cooper, R. C. Fedder, and D. P. Schumacher, Phys. Rev. 163, 506 (1967); 168, 654(E) (1968).

[12]K. R. Lea, M. J. M. Leask, and W. P. Wolf, J. Phys. Chem. Solids 23, 1381 (1962).

[13]C. Y. Huang, K. Sugawara, and B. R. Cooper, Phys. Rev. B 15, 3003 (1977).

[14]J. Kötzler, G. Raffius, A. Loidl, and C. M. E. Zeyen, Z. Phys. B 35, 125 (1979).

[15]R. Siemann and B. R. Cooper, Phys. Rev. Lett. 44, 1015 (1980).

[16]B. R. Cooper, J. Magn. Magn. Mater. 29, 230 (1982).

[17]H. Bartholin, I. S. Jacobs, B. R. Cooper, and O. Vogt, Bull. Phys. Soc. 17, 249 (1972).

[18]H. Bartholin, D. Florence, Wang Tcheng-Si, and O. Vogt, Phys. Status Solidi A 24, 631 (1974).

[19]H. Bartholin, D. Florence, Wang Tcheng-Si, and O. Vogt, Phys. Status Solidi A 29, 275; also see the remanent magnetization behavior for CeSb given in J. Rossat-Mignod, P. Burlet, J. Villain, H. Bartholin, Wang Tcheng-Si, D. Florence, and O. Vogt, Phys. Rev. B 16, 440 (1977).

[20]The values of T_N and Δ from previous work for the cerium monopnictides are taken from B. R. Cooper, in *Magnetism in Metals and Metallic Compounds,* edited by J. T. Lopuszanski, A. Pekalski, and J. Przystawa (Plenum, New York, 1976), pp. 225–263. Original sources are quoted in Cooper's paper. The value of Δ for CeP is, however, the more recent value found in H. Heer, A. Furrer, and W. Halg, J. Magn. Magn. Mater. 3, 55 (1976).

[21]G. Busch and O. Vogt, Phys. Lett. 20, 152 (1966).

[22]The Bloch equations are not appropriate when H is smaller than, or comparable to, the rf field, and hence, when $H=0$. In our case the rf field is $\sim 10^{-2}$ G, and is much smaller than the fields of interest (>10 G). Consequently the Bloch equations are appropriate to describe our system.